Processing and structure-property relationships of natural rubber/wheat bran biocomposites

Krzysztof Formela[1,*], Aleksander Hejna[1], Łukasz Piszczyk[1], Mohammad Reza Saeb[2], Xavier Colom[3]

[1]Department of Polymer Technology, Gdansk University of Technology, Gdansk, Poland
[2]Department of Resin and Additives, Institute for Color Science and Technology, Teheran, Iran
[3]Department of Chemical Engineering, Universitat Politècnica de Catalunya Barcelona Tech, Terrassa, Spain

[*]Corresponding author: Dr. Krzysztof Formela, Department of Polymer Technology, Faculty of Chemistry, Gdansk University of Technology, G. Narutowicza Str. 11/12, PL 80-233, Gdansk, Poland. e-mail: krzysztof.formela@pg.gda.pl ; kformela.ktp@gmail.com

Abstract

In this paper, wheat bran (WB) was used as potential lignocellulose filler in biocomposites based on natural rubber (NR). For better characterization of interfacial interactions between NR and WB obtained results were compared with properties of biocomposites filled with commercial available lignocellulose fillers – wood flour (WF) and microcellulose (MC). Physical and chemical properties of each lignocellulose fillers were determined. The impact of lignocellulose filler content (ranging from 10 to 50 phr) on processing, structure, dynamic mechanical properties, thermal properties, physico-mechanical properties and morphology was investigated.

The conducted investigations showed WB could be successfully applied as a alternative and low-cost substitute of lignocellulose fillers in wood polymer composites.

Keywords: Lignocellulose fillers; Natural rubber; Biocomposites; Processing; Structure-property relationships

1. Introduction

Limited petroleum resources, continuously increasing amount of polymeric waste and higher awareness of the society, are the main economic and environmental factors caused dynamic development of biodegradable polymeric materials. Estimated data indicate that production and further application of biodegradable polymers in different branches of industry will grow by over 30 % annually, which confirm their variety of potential applications [Shen L, Haufe J, Patel MK (2009) Product Overview and Market Projection of Emerging Biobased Plastics. Report No: NWS-E-2009-32 The Netherlands: Utrecht]. Therefore, searching for new biodegradable polymers and biocomposites with tailored performance properties [Kwiecień I, Adamus G, Bartkowiak A, Kowalczuk M (2104) Synthesis and structural characterization at the molecular level of oligo(3-hydroxybutyrate) conjugates with antimicrobial agents designed for food packaging materials. Des. Monomers Polym. 17: 311-321. //// Franciszczak P, Błędzki AK (2015) Tailoring of dual-interface in high tenacity PP composites – Toughening with positive hybrid effect. Compos. Part A: Appl. S. doi:10.1016/j.compositesa.2015.07.001.] and suitable low price [Chikhi M, Agoudjil B, Boudenne A, Gherabli A (2013) Experimental investigation of new biocomposite with low cost for thermal insulation. Energ. Buildings 66:267-273. //// Korol J, Lenża J, Formela K (2015) Manufacture and research of TPS/PE biocomposites properties. Compos. Part B: Eng. 68:310-316 /// Sałasińska K, Ryszkowska J (2015) The effect of filler chemical constitution and morphological properties on the mechanical properties of natural fiber composites. Compos. Interfaces 22:39-50.] are the subjects of research conducted nowadays in many academic and industrial scientific centers in the world.

Special group of biocomposites are wood polymer composites (WPCs). WPCs are refer as a materials consisting of one or more lignocellulosic filler and one or a mixture of polymers. High amount of cellulose rich by-products generated from wood and agriculture industry, can be successfully applied as biofillers in polymeric matrix, which reduce material costs and provide specific properties of biocomposites e.g. low density, high stiffness, corrosion resistance, harmlessness, renewable characteristics and biodegradability [Sobczak L, Brüggemann O, Putz RF (2013) Polyolefin Composites with Natural Fibers and Wood-Modification of the Fiber/Filler–Matrix Interaction. J. Appl. Polym. Sci. 127:1-17. //// Gurunathan T, Mohanty S, Nayak SK (2015) A review of the recent developments in biocomposites based on natural fibres and their application perspectives, Compos. Part A: Appl. S. 77: 1-25. ////Mohammed L, Ansari MNM, Pua G, Jawaid M, Islam MS (2015) A review on natural fiber reinforced polymer composite and its applications. Int. J. Polym. Sci.

Article ID 243947]. Above mentioned factors caused that WPCs are commonly used as building and automobile products, as environmental friendly alternative for neat polymers [Korol J, Burchart-Korol D, Pichlak M (2015) Expansion of environmental impact assessment for eco-efficiency evaluation of biocomposites for industrial application. J. Clean. Prod. doi: 10.1016/j.jclepro.2015.11.101 /// Teuber L, Osburg VS, Toporowski W, Militz H, Krause A (2016) Wood polymer composites and their contribution to cascading utilization. J. Clean. Prod. 110:9-15].

It is well known that performance properties of WPCs depend on the physical and chemical interactions between polymer matrix and lignocellulose filler. Matrix-filler interactions level is affected by polymer matrix and characteristics of lignocellulose fillers. Many attempts were recently focused on influence of lignocellulose fillers characteristics on processing and structure-property relationships of WPCs. Liu et al. [Liu R, Peng Y, Cao J, Chen Y (2014) Comparison on properties of lignocellulosic flour/polymer composites by using wood, cellulose, and lignin flours as fillers. Compos. Sci. Technol. 103, 1-7.] applied wood flour, lignin flour and cellulose flour (the last two were separated from wood flour) in biocomposites based on poly(propylene) (PP) or poly(lactic acid) (PLA) as matrix. The results confirmed that chemical composition of lignocellulosic flour had significant influence on physical, mechanical and thermal properties of biocomposites, which were also related to type of used polymer matrix.

Peltola et al. [Peltola H, Pääkkönen E, Jetsu P, Heinemann S (2014) Wood based PLA and PP composites: Effect of fibre type and matrix polymer on fibre morphology, dispersion and composite properties. Compos. Part A: Appl. S. 61:13-22.] used five types of lignocellulose fillers (wood flour, thermo-mechanical spruce pulp fibers and three types of chemically bleached kraft pulp fibers) as reinforcement of poly(propylene) or poly(lactic acid) matrix. Presented results indicate that lignocellulose fibers disperse better into PLA than in PP as a matrix. The best performance properties was determined for PLA composites reinforced with thermo-mechanical spruce pulp (TMP) fibers. It was related to stiffness of TMP fibers and lignin present in TMP, which might acts like as compatibilizer between PLA matrix and the fibre phase. Furthermore, obtained results shown that in comparison to lignocellulose fibres, lignocellulose flour is not reinforcing polymeric matrix.

Faludi et al. [Faludi G, Dora G, Imre B, Renner K, Móczó J, Pukánszky B (2014) PLA/lignocellulosic fiber composites: Particle characteristics, interfacial adhesion, and failure mechanism. J. Appl. Polym. Sci. 131: 39902.] used six different commercially available lignocellulosic fibers (four wood fibers, microcrystalline cellulose, grinded corn cob) with

varying chemical composition and particle characteristics to prepare biocomposites based on poly(lactic acid) (PLA). Presented results suggest strong interfacial adhesion between PLA matrix and lignocellulosic fibers. It was observed that reinforcement effect was related to size and aspect ratio of lignocellulosic fibers and surprisingly independent of their origin (chemical composition).

Błędzki et al. [Błędzki AK, Franciszczak P, Osman Z, Elbadawi M (2015) Polypropylene biocomposites reinforced with softwood, *abaca*, jute, and kenaf fibers. Ind. Crop. Prod. 70:91-99.] characterized biocomposites based on PP reinforced with softwood, *abaca*, jute and kenaf fibers. Presented results indicate that final properties of biocomposites are related to the mechanical properties and geometry of fibers.

Berthet et al. [Berthet MA, Angellier-Coussy H, Machado D, Hilliou L, Staebler A, Vicente A, Gontard N (2015) Exploring the potentialities of using lignocellulosic fibres derived from three food by-products as constituents of biocomposites for food packaging. Ind. Crop. Prod. 69, 110-122] studied the composites based on poly(3-hydroxybutyrate-co-valerate) (PHBV) filled with three different agricultural waste (wheat straw, brewing spent grains and olive mills). It was found that chemical composition of lignocellulose filler might has have influenced on their grinding ability and their processing with PHBV during extrusion. Appliction of lignocellulose fillers into PHBV matrix caused deterioration of mechanical properties, which was related to: weak adhesion between PHBV matrix and lignocellulose fillers phase, decrease crystallinity of PHBV and thermo-mechanical degradation of polymer chain during processing.

Georgiopoulos and Kontou [Georgiopoulos P, Kontou E (2015) The effect of wood-fiber type on the thermomechanical performance of a biodegradable polymer matrix. J. Appl. Polym. Sci. 132:42185.] evaluate the thermo-mechanical properties of poly(butylene adipate-terephthalate)/poly(lactic acid) (PBAT/PLA) blends modified with three different types of commercial available wood-fibers (soft wood from selected conifers and two types of raw cellulose). The results shown that final properties of PBAT/PLA blends are related to type of lignocellulose fillers and its content. It was observed that biocomposites filled with 20 % of soft wood from selected conifers attain predominant properties, while application of raw cellulose is more suitable for biocomposites with higher weight fractions of lignocellulose filler.

The present state of knowledge shows that detailed characteristics of lignocellulose filler can be valuable tool during tailoring of biocomposites with desired performance properties. However, the present research in this field are focused mainly on thermoplastic

biocomposites based on polyolefins or biodegradable aliphatic polyesters as matrix, while correlations between lignocellulose fillers characteristics and selected properties of elastomeric matrix is poorly described in the literature. A comprehensive literature overview about elastomeric composites with lignocellulose fillers was recently presented by Zhou et al. [Zhou Y, Fan M, Che L, Zhuang J (2015) Lignocellulosic fibre mediated rubber composites: An overview. Compos. Part B: Eng. 76:180-191]

In the present work the potential of wheat bran (WB) as a lignocellulose filler in biocomposites with natural rubber (NR) matrix was evaluated. Wheat bran is food industry solid by-products, which can be applied as cheap, eco-friendly and cellulose rich biofiller. However, only a few recently published papers concerned using of WB in polymer composites [Błędzki AK, Franciszczak P, Mamun A (2014) The utilization of biochemically modified microfibers from grain by-products as reinforcement for polypropylene biocomposite. Express Polym. Lett. 10: 767-778 //// Hejna A, Formela K, Saeb MR (2015) Processing, mechanical and thermal behavior assessments of polycaprolactone/agricultural wastes biocomposites. Ind. Crop. Prod. 76:725-733.]. In the light of above mentioned studies, we aimed to examine the effects of the WB content (in range: 10-50 phr) on curing characteristics, chemical structure (FTIR analysis), thermal properties (TGA), dynamic mechanical properties (DMA) static mechanical properties (tensile strength, elongation at break, hardness), physical properties (density, cross-link density, sol fraction), and morphology (SEM) of NR/WB biocomposites. Furthermore, for comprehensive structure-properties relationships assessment and better understanding the interfacial interactions between NR and WB, the characteristics of NR/WB biocomposites were compared with properties of biocomposites filled with commercial available lignocellulose fillers: wood flour (WF) and microcellulose (MC).

2. Experimental

2.1. Materials

Natural rubber (NR) type RSS with density 0.92 g/cm^3 was supplied by Guma-Pomorska (Poland).

Wheat bran (WB) was purchased from Młyn Gospodarczy Sp. J. (Poland). WB biofiller, prior to processing, were dried at 80 °C and then mechanically grinded in a co-rotating twin-screw extruder at 180 °C to obtain particles with a narrow size distribution. Wood flour (WF) Arbocel C350 and microcellulose (MC) Arbocel B800 were purchased from Rettenmaier and Söhne GmbH (Germany). WF and MC were used as received.

Vulcanization accelerators (TBBS - N-tert-butyl-2-benzothiazole sulfonamide, TMTD - tetramethylthiuram disulfide), stearic acid, zinc oxide and sulfur with technical purity were supplied by Standard Sp. z o.o. (Poland).

2.2. Biocomposites preparation

Biocomposites were prepared at 70 °C using a Brabender batch mixer model GMF 106/2. The rotational speed of rotors was 100 rpm. The mixing time equaled 8 minutes which included 2 minutes of preliminary plasticization of natural rubber, 4 minutes of mixing with the lignocellulose fibers (WB, WF or MC) and 2 minutes of mixing the blend with the sulfur curing system. The lignocellulose fibers content in the biocomposites was altered from 10 to 50 parts per hundred of rubber (phr). For all samples the same curing system samples was used. The curing system composition (phr): zinc oxide 5.0; stearic acid 3.0; TBBS 1.0; TMTD 0.25; sulfur 2.0.

The obtained composites were compression molded into 2-mm thick samples at 150 °C and 4.9 MPa according to determined optimal vulcanization time. Unfilled natural rubber processed in the same conditions was used as reference sample.

2.3. Measurements

Elemental analysis (C, H, N, S) of lignocellulose fillers were carried out using a Flash 2000 CHNSO Analyser from Thermo Scientific (USA).

Macro- and microelements content in lignocellulose filler was determined by wavelength dispersive X-ray fluorescence spectrometry (WD-XRF) using a spectrometer S8 Tiger 1KW from Bruker (USA).

Curing characteristics was investigated according to ISO 3417 at 150 °C, using Monsanto R100S rheometer with oscillating rotor (USA). The rotor oscillation angle was 1°, while torque ranged between 0 and 100 dNm. Cure rate index values were calculated in accordance with the formula [Menon ARR, Pillai CKS, Nando GB (1998) Vulcanization of natural rubber modified with cashew nut shell liquid and its phosphorylated derivative - a comparative study, Polymer 39:4033-4036.] (1):

$$\mathrm{CRI} = \frac{100}{t_{90} - t_2} \quad (1)$$

where: t_{90} – optimum vulcanization time, min; t_2 – scorch time, min.

Chemical structure of lignocellulose fillers and biocomposites was determined using Fourier transform infrared spectroscopy (FTIR) analysis performed by means of a Nicolet

iS10 spectrometer from Thermo Scientific (USA). The device had an ATR attachment with a diamond crystal. Measurements were performed with 1 cm^{-1} resolution in the range 650-4000 cm^{-1}.

Tensile strength and elongation at break of the obtained vulcanizates were tested according to the standard ISO 37 using a Zwick Z020 testing machine (Germany) with cell load capacity of 20 kN. Tensile tests were performed at a cross-head speed of 500 mm/min. Direct extension measurements were conducted periodically using an extensometer with sensor arms. Hardness was determined using a Zwick 3130 durometer Shore A (Germany) in accordance with the standard ISO 7619-1. The reported results are the means of 5 measurements per sample.

Dynamic mechanical analysis was performed using DMA Q800 TA Instruments apparatus (USA). Samples cut to the dimensions of 40 x 10 x 2 mm were loaded with a variable sinusoidal deformation force in the single cantilever bending mode at the frequency of 1 Hz under the temperature rising rate of 4°C/min within the temperature range between -70 and 20°C.

Swelling degree of biocomposites (0.2 g samples) as function of time was determined by equilibrium swelling in toluene (room temperature). Swelling degree was calculated in accordance with the formula (2):

$$Q = \frac{m_t - m_o}{m_o} \times 100\% \quad (2)$$

where: Q – swelling degree; m_t – mass of the sample swollen after time t, g; m_o – initial mass of sample, g.

Cross-link density of the biocomposites was determined by equilibrium swelling in toluene (room temperature, 72 h), according to the Flory-Rehner equation [Flory PJ, Rehner J (1943) Statistical mechanics of cross-linked polymer networks I. rubberlike elasticity. J Chem Phys 11:512-520.] (3):

$$v_e = \frac{-[\ln(1 - V_r) + V_r + \chi V_r^2]}{[V_1(V_r^{1/3} - V_r/2)]} \quad (3)$$

where:

v_e – cross-link density, mol/cm^3; V_r – gel volume in the swollen sample; V_1 – solvent molar volume (toluene = 106.2, cm^3/mol); χ – polymer-solvent interaction parameter (in the calculations, it was assumed to be 0.393 [López-Manchado MA, Herrero B, Arroyo M (2003)

Preparation and characterization of organoclay nanocomposites based on natural rubber. Polym. Int. 52:1070–1077.]).

The Flory-Rehner equation can be applied for non-filled compounds, while studied samples contain lignocellulose fillers. Kraus correction for filled compounds [Kraus GJ (1963) Swelling of filler-reinforced vulcanizates. J Appl Polym Sci 7:861-871] was applied in order to calculate the actual remaining crosslink density. Cross-link density with Kraus correction was calculated according equations (4) and (5):

$$v_{\text{after correction}} = \frac{v_e}{1 + \mathrm{K} + \Phi} \quad (4)$$

$$\Phi = \frac{\phi_f \times \rho_r \times m_0}{\rho_f \times m_{dry}} \quad (5)$$

where:

v_e – the measured chemical cross-link density, mol/cm^3; $v_{\text{after correction}}$ – the actual chemical cross-link density, mol/cm^3; K – constant characteristic of the filler but independent of the solvent; ϕ_f – the volume fraction of filler in the sample which is calculated; ρ_r – the density of studied compound, g/cm^3; m_0 – the weight of sample before extraction, g; ρ_r – the density of filler, g/cm^3; m_{dry} – the weight of sample after extraction, g

Sol fraction was determined as mass difference of biocomposites before swelling (W_1) and after extraction (W_2), according to equation (6):

$$\text{Sol fraction} = \frac{W_1 - W_2}{W_1} \times 100\,\% \quad (6)$$

The density of the samples was measured based on the Archimedes method, as described in ISO 2781. Accordingly, all measurements were carried out at room temperature in methanol medium.

Thermogravimetric analysis (TGA) was performed on a NETZSCH TG 209 apparatus. Samples of biocomposites weighing approx. 5-mg were placed in a corundum dish. The measurement was conducted in the temperature range 25-600 °C and under nitrogen atmosphere, at a heating rate of 20 °C/min.

The morphology of biocomposites after extraction in toluene (at room temperature, 72 h) was observed with a JEOL 5610 scanning electron microscope. Before measurement the samples were covered with a fine gold-palladium layer in order to increase their conductivity in a vacuum chamber.

3. Results and discussion

3.1. Characteristics of lignocellulose fillers

The chemical composition of WB, WF and MC determined by elemental analysis and WD-XRF analysis are presented in Table 1. Based on literature data [Caprez A, Arrigoni E, Amadò R, Neukom H (1986) Influence of different types of thermal treatment on the chemical composition and physical properties of wheat bran. J. Cereal Sci. 4:233-239] and presented results, noticeable difference between WB and other applied biofillers is content of proteins, which was confirmed by the nitrogen content. Furthermore, wheat bran was characterized by higher content of macro- and microelements, which could enhanced activity of enzymes and microorganisms during biodegradation of biocomposites [Tomaszewska-Ciosk E, Golachowski A, Zdybel E (2013) Determination of biodegradation rate of carrier for microorganism immobilization fabricated based on starch. Pol. J. Chem. Tech. 15:110-114]. This phenomenon should be evaluated in further studies on this field.

The particle size distribution and the appearance of the used lignocellulose fillers are presented in Fig. 1. Size of filler imposes a significant influence on its disperseability in the polymer matrix. MC filler was characterized by the smallest size with ~80% wt. of particles below 0.13 mm. It was observed that dimensions of WB filler particles (~ 100 wt. of particles below 0.50 mm) was slightly higher comparing to WF particles (~ 95 wt. of particles below 0.50 mm). This suggests that using a co-rotating twin screw extrusion is effective grinding method of wheat bran, which could be applied in industry.

Table. 1. Elemental analysis of applied lignocellulose fillers

Element	Method	WB	WF	MC
		Element content, wt.%		
C	Elemental analysis	44.92	48.20	43.89
H		6.26	5.82	6.12
N		2.48	1.06	0.43
K	WD-XRF	1.26	0.14	-
P		0.62	-	-
Mg		0.22	-	-
S		0.14	0.03	0.02
Ca		0.08	0.16	0.04
Cl		0.07	-	-
Fe		0.01	0.02	-
Si		-	0.19	-

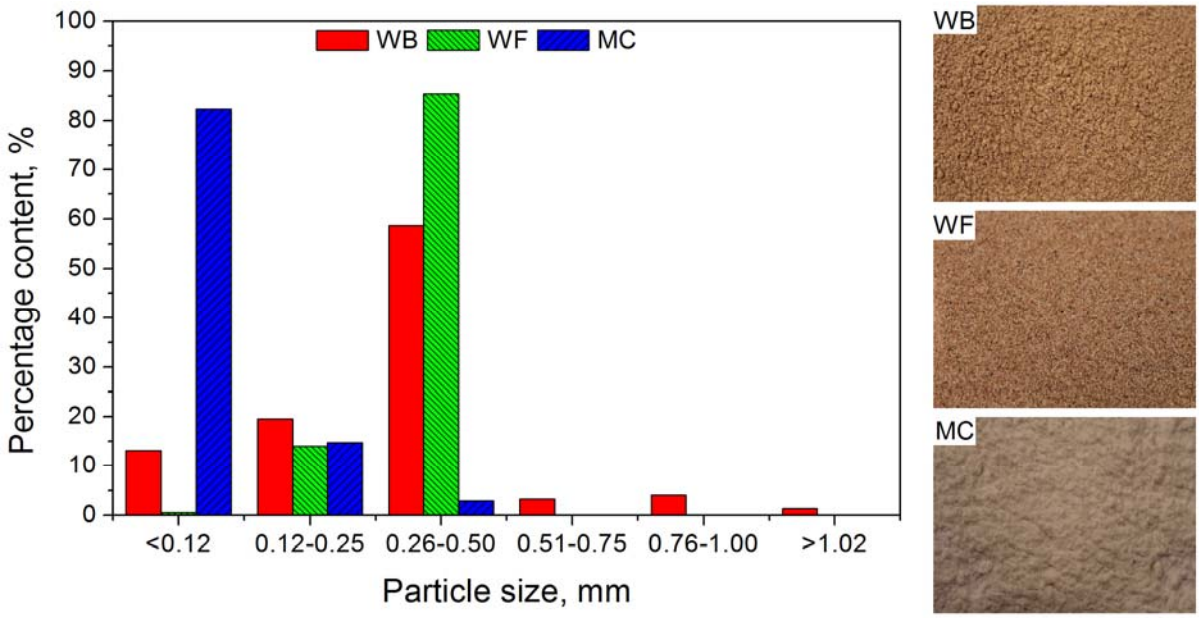

Figure 1. The particle size distribution and appearance of used lignocellulose fillers

FTIR spectra of applied lignocellulose fillers are presented in the Figure 2. Similarities in spectra for all fillers are related to the chemical composition of used materials. Signal (a) characteristic for stretching vibrations of hydroxyl groups was observed at 3300-3350 cm^{-1}. The bands (b) in the range of 2940-2860 cm^{-1} were attributed to the symmetric and asymmetric stretching vibrations of C-H bonds in CH_2 groups present in aliphatic chains and CH_3 end groups. Absorbance maxima around 1740 and 1640 cm^{-1} (signals c and d), could be associated with the stretching vibrations of unconjugated C=O and C=C bonds in cellulose, hemicellulose and lignin (Yona AMC, Budija F, Kricej B, Kutnara A, Pavlic M, Pori P, Tavzes C, Petric M (2014) Production of biomaterials from cork: Liquefaction in polyhydric alcohols at moderate temperatures. Ind. Crop. Prod. 54:296-301). The absorption band (e) around 1510 cm^{-1} was related to the stretch of aromatic rings present in lignin (Colom X, Carrillo F, Nogués F, Garriga P (2003) Structural analysis of photodegraded wood by means of FTIR spectroscopy. Polym. Degrad. Stab. 80:543-549.), therefore this peak band was not observed for microcellulose. Signal (f) around 1460 cm^{-1} can be associated with CH_2 and HOC in-plane bending vibrations, characteristic for carbohydrates (Ciolacu D, Ciolacu F, Popa VI (2011) Amorphous cellulose - structure and characterization. Cellul. Chem. Technol. 45:13-21). Signal (g) in the range of 1360-1310 cm^{-1} is related to the OH groups plane deformation vibrations, while band (h) at 1230 cm^{-1} is attributed to the stretching of C-O and C=O bonds (Schwanninger M, Rodrigues JC, Pereira H, Hinterstoisser B (2004) Effects of short-time vibratory ball milling on the shape of FT-IR spectra of wood and cellulose, Vib.

Spectrosc. 36:23-40). In the range of 1160-1010 cm^{-1} there are present the absorption bands (i) and (j), which are characteristic for asymmetric stretching vibrations of C-O-C groups and C-O, C=C and C-C-O stretching, respectively [Xu F, Yu J, Tesso T, Dowell F, Wang D (2013) Qualitative and quantitative analysis of lignocellulosic biomass using infrared techniques: A mini-review. Appl. Energy 104:801-809.]. The intensity of band (i) at 1010 cm^{-1} is very sensitive to the degree of crystallinity of cellulose, which is related to changes in angles around β-1,4-glycosidic linkages and possible reorganization of hydrogen bond in cellulose [Proniewicz LM, Paluszkiewicz C, Wesełucha-Birczyńska A, Majcherzyk H, Barański A, Konieczna A (2001) FT-IR and FT-Raman study of hydrothermally degradated cellulose. J. Mol. Struct. 596:163-169.]. Presented results show that wood flour contains mainly amorphous cellulose, while its crystalline form is presented in microcellulose and wheat bran. Amorphous form of wood flour can be due to diverse type of wood used during preparation of this lignocellulose filler. On the other hand, high content of crystalline form cellulose in thermo-mechanically milled wheat bran could be surprising. This suggests that heat and mechanical stress acting on wheat bran during short-time extrusion is not suitable for transformation of crystalline cellulose into its amorphous form. Similar observations were described in works [Caprez A, Arrigoni E, Amadò R, Neukom H (1986) Influence of different types of thermal treatment on the chemical composition and physical properties of wheat bran. J. Cereal Sci. 4:233-239. //// Agarwal UP, Reiner RS, Ralph SA (2010) Cellulose I crystallinity determination using FT-Raman spectroscopy: univariate and multivariate methods. Cellulose 17:721-733.]. Furthermore, wheat bran contains proteins with amide and carbonyl groups. These polar groups are able to enhanced formulation of hydrogen bonds into cellulose, which could affecting its crystallinity. Signal (k) observed around 890 cm^{-1} is attributed to the bending vibrations of C-H bonds in carbohydrate structure of used biofillers (Faix O (1991) Classification of Lignins from Different Botanical Origins by FT-IR Spectroscopy. Holzforschung 45:21-27).

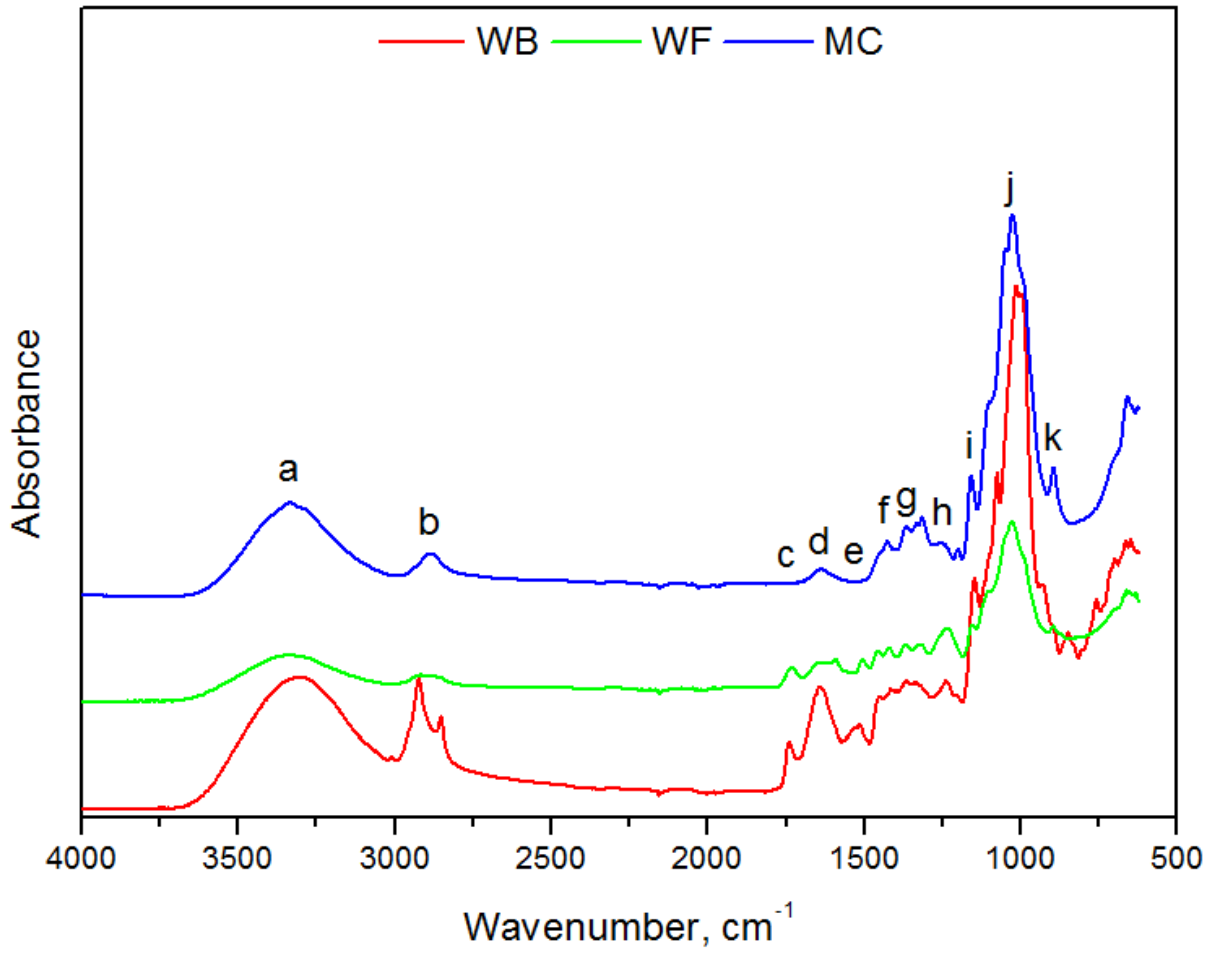

Figure 2. FTIR spectra of used lignocellulose fillers

3.2. Curing characteristics

The influence of lignocellulose fillers content on curing characteristics of NR/lignocellulose filler biocomposites is shown in Table 2 and Figure 3.

Table 2. Curing characteristics of biocomposites

Component	Sample									
Natural rubber (NR)	100	100	100	100	100	100	100	100	100	100
Wheat bran (WB)	-	10	30	50						
Wood flour (WF)					10	30	50			
Microcrystalline cellulose (MC)								10	30	50
Curing characteristiscs at 150 °C										
Minimal torque (dNm)	2.4	1.7	2.2	2.6	2.5	2.9	2.4	2.9	7.7	11.7
Maximal torque (dNm)	24.0	24.4	31.2	37.4	28.4	34.3	39.6	29.2	39.7	47.5
ΔM (dNm)	21.6	22.7	29.0	34.8	25.9	31.5	37.2	26.3	32.0	35.8
Scorch time (t_2, min)	5.8	5.9	5.1	5.3	5.7	5.3	5.1	1.3	1.0	0.9
Optimum cure time (t_{90}, min)	7.5	8.2	8.2	8.7	7.9	7.6	7.6	3.2	3.3	3.5
Cure rate index (CRI, min^{-1})	58.8	43.5	32.3	29.4	45.5	43.5	40.0	52.6	43.5	38.5

It was observed that curves for NR/WB and NR/WF biocomposites shown similar trend, while curing behavior of NR/MC was clearly different. The increase of wheat bran or wood flour content in NR based biocomposites had insignificant impact on minimal torque. This suggests good processing properties of the highly filled (50 phr of lignocellulose filler) NR/WB and NR/WF biocomposites, which was comparable to unfilled NR. On the other hand, higher content of microcellulose in NR/MC biocomposites caused increase of minimal torque values. This indicates worse incorporation of MC in natural rubber matrix, which was related to lower particles size of this filler comparing to WB and WF (see Figure 1). Maximal torque and torque increment (ΔM) increase with higher content lignocellulose filler, regardless of its type. The increase of maximal torque and ΔM resulting from limited mobility of polymer chains related to NR/lignocellulose filler interactions and cross-link density of biocomposites [Jacob M, Thomas S, Varughese KT (2004) Mechanical properties of sisal/oil palm hybrid fiber reinforced natural rubber composites. Compos. Sci. Technol. 64:955-965. /// Karaağaç B (2014) Use of ground pistachio shell as alternative filler in natural rubber/styrene–butadiene rubber-based rubber compounds. Polym. Compos. 35:245-252.]. This phenomenon has significant impact on stiffness and shear modulus of biocomposites. Among all studied samples, NR/WB biocomposites were characterized by the lowest maximal torque and ΔM values. This suggests that proteins present in WB can act like plasticizers in prepared biocomposites [Selmin F, Franceschini I, Cupone IE, Minghetti P, Cilurzo F (2015) Aminoacids as non-traditional plasticizers of maltodextrins fast-dissolving film, Carbohydr. Polym. 115:613-616.], which reduced their stiffness.

In case of biocomposites filled with WB or WF, increase content of lignocellulose filler caused decrease of scorch time. Higher content of WB in NR based composites cause decrease of optimal cure time, while for NR/WF composites opposite trend was observed. It is worth to noticed that the values of obtained results were close to unfilled NR. Slight difference between NR/WB and NR/WF could be due to difference in particle size distribution (see Figure 1) and lignocellulose filler characteristics (e.g. content of proteins, sulfur or microelements - see Table 1), which could affect matrix-filler interactions, thus curing efficiency. NR/MC biocomposites were characterized by lower values of scorch time and optimal cure time comparing to unfilled NR, NR/WB and NR/WF biocomposites. This is due to small size particles of MC, which allows good dispersion of lignocellulose filler into NR matrix and improves interactions between lignocellulose filler surface and NR matrix [Sareena C, Ramesan MT, Purushothaman E (2012) Utilization of peanut shell powder as a novel filler in natural rubber. J. Appl. Polym. Sci. 125:232-234.]. It was observed that

increase content of MC in biocomposites decrease scorch time and increase of optimal cure time. It could be surprising, because according to literature the scorch time and optimal cure time of elastomeric/lignocellulose fillers composites tended to decrease consistently with increasing lignocellulose filler loading [Ismail H, Edyham MR, Wirjosentono B (2002) Bamboo fibre filled natural rubber composites: the effects of filler loading and bonding agent. Polym. Test. 21:139-144. /// Hong H, He H, Jia D, Zhang H (2011) Effect of wood flour on the curing behaviour, mechanical properties, and water absorption of natural rubber/wood flour composites. J Macromol Sci Part B Phys 50:1625-1636. /// Sareena C, Ramesan MT, Purushothaman E (2012) Utilization of coconut shell powder as a novel filler in natural rubber. J Reinf Plast Compos 31:533-547.]. This trend is explained by prolonged processing time of the biocomposites on the mills, which is necessary to obtain proper homogeneity of the material. Furthermore, increasing content of lignocellulose filler (increasing viscosity) enhanced shear forced acting on the processed material, therefore more heat is generated due to additional friction. It should be noticed that studied were obtained at elevated temperature (70 °C) using a internal mixer, which reduce the viscosity biocomposites and decrease time of their processing. Moreover, comparing to two-roll mills, using of internal mixer allows generation of different type of shear forces which affecting dispersion of components and final homogeneity of biocomposites. Regardless of type of lignocellulose filler, cure rate index (CRI) decrease with increasing content of filler. This indicate that used lignocellulose fillers hinders vulcanization of biocomposites. This phenomenon is due to possible adsorbing of the curing system (e.g. activators, accelerators) by lignocellulose fillers and limited mobility of NR molecules related to good dispersion of lignocellulose filler into NR matrix [Jiang C, He H, Jiang H, Ma L, Jia DM (2013) Nano-lignin filled natural rubber composites: Preparation and characterization. Express Polym. Lett. 7:480-493. /// Raza MA, Ashraf MA, Westwood AVK, Jamil T, Ahmad R, Inamm A, Deen KM (2014) Maleated high oleic sunflower oil-treated cellulose fiber-based styrene butadiene rubber composites. Polym. Compos. doi: 10.1002/pc.23273.]. For better presentation of biocomposites curing behavior, selected curing curves are shown in the Figure 3. It was noticed that addition of lignocellulose filler prevent adverse reversion of NR matrix, which was observed for unfilled NR during curing in prolonged time (in study case after 15 min). This phenomenon may be due to presence of phenolic compounds in lignocellulose fillers, which limit thermo-oxidation of biocomposites.

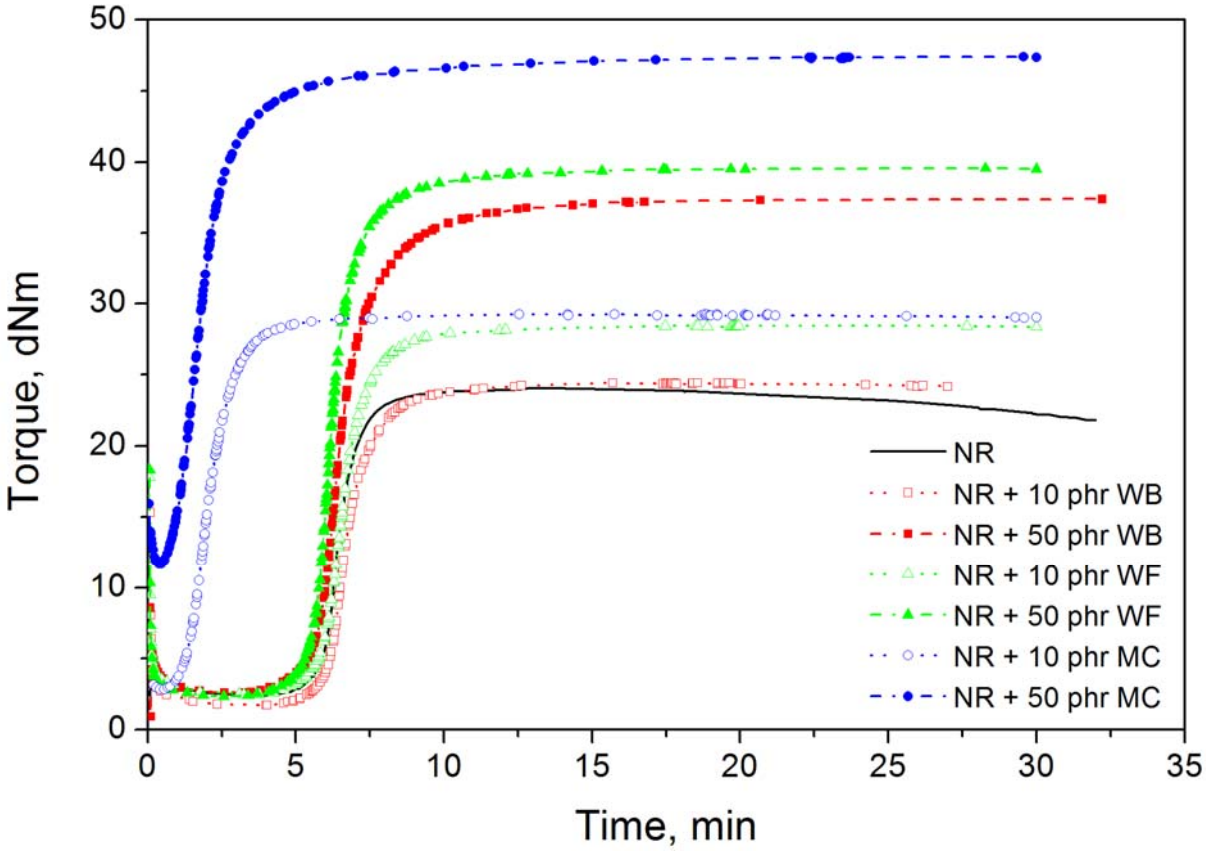

Figure 3. Curing curves for natural rubber/lignocellulose filler biocomposites

Presented results confirm significant influence of chemical composition and particles size distribution of lignocellulose fillers on curing behavior of studied biocomposites. For better understanding of NR-lignocellulose filler interactions, reinforcing activity of wheat bran, wood flour and microcellulose into studied biocomposites was evaluated using Wolff coefficient of activity – α_F. Correlation between M_{spec} and α_F was calculated according equation (7) and (8):

$$\Delta M_{spec} = \frac{\Delta M_x}{\Delta M_0} - 1 \quad (7)$$

$$\Delta M_{spec} = \alpha_F \cdot \frac{m_x}{m_p} \quad (8)$$

where:

ΔM_x – the torque increment of the vulcanizate containing x phr of filler during vulcanization (dNm); ΔM_0 – the torque increment of unfilled vulcanizate; m_x – weight of added filler (g); m_p – weight of polymer in vulcanizate (g)

The reinforcing amount of filler is defined as active for positive a_F values and inactive for negative a_F values. As presented in Fig. 4, all studied biocomposites was characterized by positive Wolff activity coefficient, which suggests reinforcing effect of applied lignocellulose fillers increase with increasing content of filler [Kramárová Z, Alexy P, Chodák I, Špirk E, Hudec I, Košíková B, Gregorová A, Šúri P, Feranc J, Bugaj P, Ďuračka M (2007) Biopolymers as fillers for rubber blends 18:135-140.]. However, this effect was less visible for NR/WB biocomposites, what confirm partial plasticizing of NR matrix by proteins present in WB.

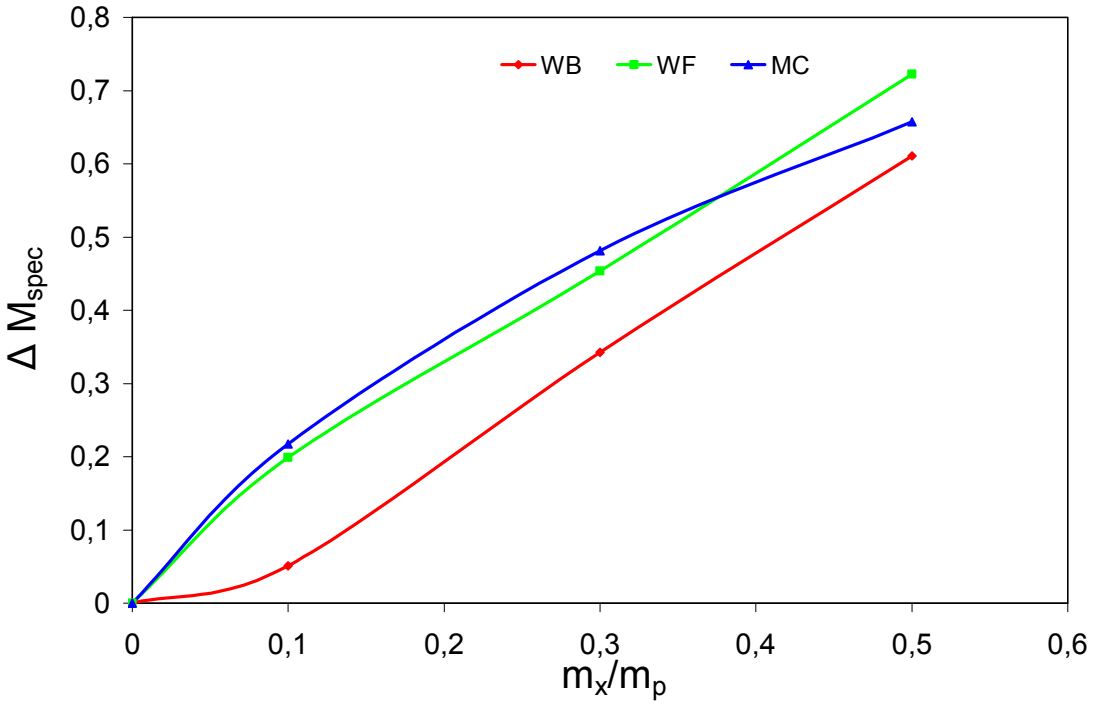

Figure 4. Dependence torque increment of biocomposites according to Wolff on filler content

3.3. Physico-mechanical properties

The results of physico-mechanical properties are presented in Table 3. As could be expected, in most cases incorporation of lignocelluloe fillers into the NR matrix caused noticeable drop in tensile strength and elongation at break. The exception is sample NR + 10 phr MC, which tensile strength and elongation at break values were comparable to unfilled NR (reference sample). This is related to small size particles of MC, which enhanced matrix-filler interactions. Furthermore, it was noticed that for highly filled NR biocomposites tensile strength and elongation at break values were comparable. Observed deterioration of mechanical properties of biocomposites, can be explained by weak compatibility between NR matrix and lignocellulose fillers. On the other hand, positive value of Wolff activity

coefficient suggest reinforcing effect of used lignocellulose fillers, which may be surprising and confusing. This phenomenon is probably due to the strain inducted crystallization of NR matrix [Brüning K, Schneider K, Heinrich G (2012) Deformation and orientation in filled rubbers on the nano- and microscale studied by X-ray scattering. J. Polym. Sci. Pol. Phys. 50:1728-1732. ///Ren Y, Zhao R, Yao Q, Li Q, Zhang X, Zhang L (2015) Effects of plasticizers on the strain-induced crystallization and mechanical properties of natural rubber and synthetic polyisoprene. RSC Adv. 5:11317-11324.]. During tensile test a part of NR turns the amorphous rubber into a semicrystalline material. Highly oriented crystallites acting like active filler particles or physical crosslinks, which increase the tensile strength. The stress-strain curves and pictures of biocomposites samples after tensile tests are presented in Fig. 5. It was observed that for NR/lignocellulose filler biocomposites strain-induced crystallization was restricted. Incorporation of higher amount of filler to NR matrix limited mobility of polymer chains and their orientation during stretching, what have significant impact on mechanical properties of obtained composites (Khan et al., 2013). Limited mobility of natural rubber chains shifted the onset of strain-induced crystallization shifted to smaller strains comparing to unfilled NR. These corresponded with “whitening” visible on samples after tensile tests and increasing values of modulus at 100% and 300% determined for biocomposites. Limited strain-induced crystallization of NR matrix, explain also insignificant influence of chemical composition and particles size distribution of applied lignocellulose fillers on static mechanical properties of NR biocomposites filled with 50 phr of lignocellulose filler, which in studied case were comparable. Furthermore, it can be seen that increasing the amount of incorporated filler results in enhanced hardness of the biocomposites. This confirms increased stiffness of the biocomposites due to limited mobility of NR chains. It was noticed that higher content of cellulose present in lignocellulose filler resulted in improvement of biocomposites hardness, while the presence of proteins (sample NR/WB) in lignocellulose filler caused opposite effect. Summing up, differences between mechanical properties of biocomposites filled with WB, WF and MC are related to the physical state of cellulose present in filler particles (more crystalline structure in WB and MC), presence of proteins (WB) and particle size distribution of used fillers (see Figures 1 and 2).

Table 3. Physico-mechanical properties of the biocomposites.

Component	Sample									
Natural rubber (NR)	100	100	100	100	100	100	100	100	100	100
Wheat bran (WB)	-	10	30	50						
Wood flour (WF)					10	30	50			
Microcrystalline cellulose (MC)								10	30	50
Physico-mechanical properties										
Tensile strength (MPa)	20.5 ±1.6	14.0 ±0.9	12.4 ±0.4	7.2 ±0.7	16.2 ±1.3	12.2 ±1.1	6.2 ±0.5	19.4 ±2.0	10.9 ±1.4	7.0 ±0.5
Elongation at break (%)	674 ±34	675 ±19	621 ±59	534 ±31	652 ±23	646 ±15	587 ±17	694 ±35	608 ±26	527 ±18
Modulus at 100 % (MPa)	0.741	0.874	1.287	1.857	0.994	1.504	1.552	1.026	1.568	1.753
Modulus at 300 % (MPa)	1.992	1.853	2.363	2.873	2.079	2.310	2.099	2.269	2.589	2.772
Hardness (°Sh A)	46	50	59	66	54	61	68	54	62	70
Experimental density (g/cm^3)	0.950	0.977	1.031	1.069	0.977	1.025	1.051	0.983	1.044	1.075
Theoretical density (g/cm^3)	-	0.987	1.045	1.089	0.994	1.063	1.115	1.004	1.089	1.153
Porosity (%)	-	1.027	1.376	1.847	1.692	3.731	6.112	2.070	4.242	7.275
Cross-link density (mol/cm^3 × 10^{-4})	0.99	0.84	1.02	1.17	0.91	0.95	0.95	0.97	0.99	1.20
Sol fraction (%)	3.2	3.3	3.2	3.1	3.1	2.9	2.4	3.1	2.8	2.3

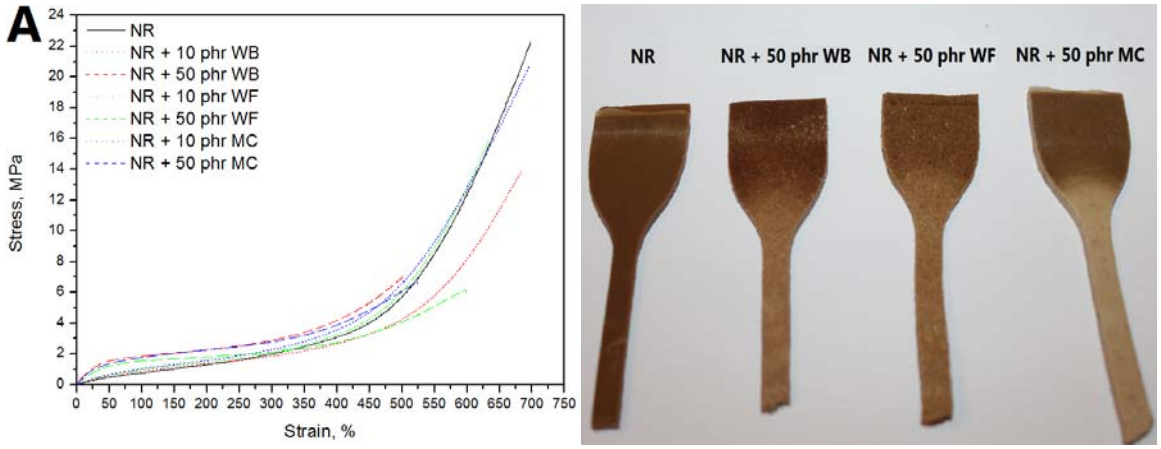

Figure 5. A - Stress-strain curves determined for biocomposites; B - samples after tensile tests

Theoretical and experimental values of density of composites filled with different amount of lignocellulose filler are shown in the Table 3. Theoretical density of composites was calculated using the equation (9):

$$\rho_C = \rho_{NR}(1-X) + \rho_F X \quad (9)$$

where ρ_C is the density of the composite, ρ_{NR} is the density of the natural rubber, ρ_F is the density of the filler and X is the fraction of the filler. Using the theoretical and experimental values of the density, values of composite's porosity were also calculated according to formula (10):

$$p = (\rho_{theo} - \rho_{\exp}) / \rho_{theo} \times 100\% \quad (10)$$

where p is the porosity of the material, ρ_{theo} is the theoretical value of density and ρ_{exp} is the experimental value of density of biocomposite.

Differences in the densities between composites are related to the applied fillers and porosity of studied biocomposites. The ascending trend in the density of green composites prepared in this work upon filler content is in good agreement with previous studies (Datta and Głowińska, 2011; Li et al., 2008). The highest values were noticed for NR/MC composites, which was expected considering the density of fillers (podać wartości dla poszczególnych napełniaczy). NR/WB samples showed higher values of density in comparison to NR/WF materials, which was not correlated with the theoretical values. Such phenomenon can be associated with different porosity of biocomposites. It can be seen that incorporation of wheat bran into natural rubber matrix resulted in the lowest value of porosity, which can be related to the chemical composition of applied fillers. In contrast to wood flour and microcellulose, wheat bran contains significant amount of starch, proteins or lipids, which can act like plasticizers, simultaneously enhancing the molecular motion and facilitating the fitting of WB particles into pores between polymer chains (Stein and Greene, 1997; Stein et al., 1999; Selmin et al. 2015/// nasz krops).

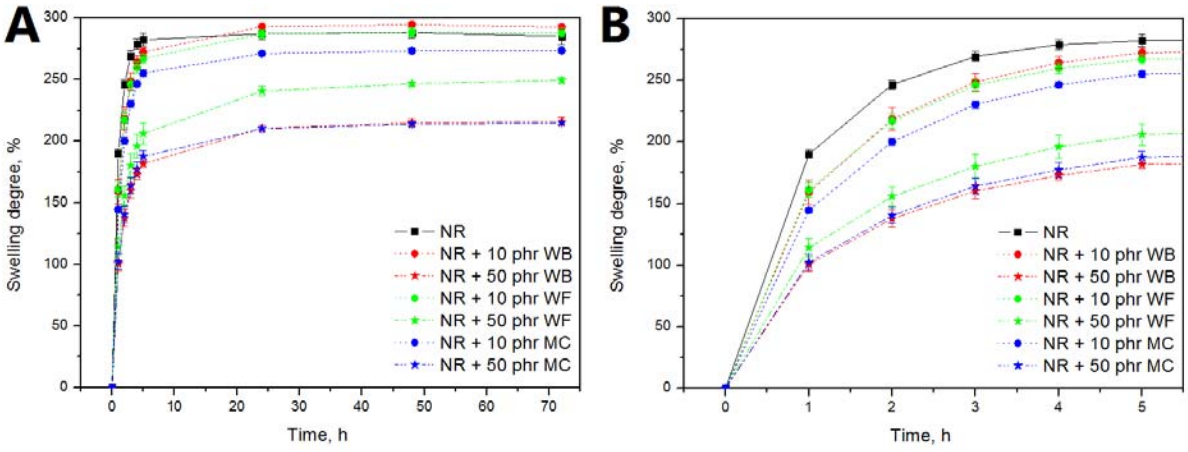

Figure 6. Swelling degree of biocomposites as function of time (swelling conducted in toluene at room temperature).

In the Fig. 6 there are shown plots of swelling degree of biocomposites in toluene are presented. For all studied samples rapid absorbance of solvent is observed during the first hours of immersion, later slowing and reaching the plateau after 48-72 h. Therefore it can be stated that analyzed materials follow Fickian behavior [Shen, C. H.; Springer, G. S. J. Comp. Mater. 1976, 10, 2.]. It can be seen that the incorporation of lignocellulose fillers decreased

the uptake of toluene in all analyzed samples, which indicates increasing cross-link density of biocomposites. However, it should be mentioned that determined swelling curves not include the volume of fillers present in biocomposites, which has a significant influence on cross-link density. Therefore, cross-link density with Kraus correction and sol fraction values are presented in Table 3. It was observed that cross-link density of biocomposites increase with increasing content of lignocellolose filler, which correspond with the results of swelling and sol fraction. Comparing to WB and MC, increase content of WF in biocomposites has small impact on change of their cross-link density. This phenomenon could be related to higher content of amorphous cellulose in this type of filler (see Figure 2), which may affects matrix-filler interactions. Samples modified with wheat bran particles showed slightly higher values of sol fraction than NR biocomposites filled with WF or MC. This is due to higher content of nonstructural wood constituents [Horvath AL (2006) Structurally Complicated Materials: I. Wood. J Phys. Chem. Ref. Data 35:77-92.] in wheat bran comparing to wood flour or microcellulose (see Table 1).

3.4. FTIR analysis

Based on economic and environmental aspects, further research was performed for biocomposites with the highest (50 phr) content of lignocellulose fillers, which showed satisfactory processing and physico-mechanical properties.

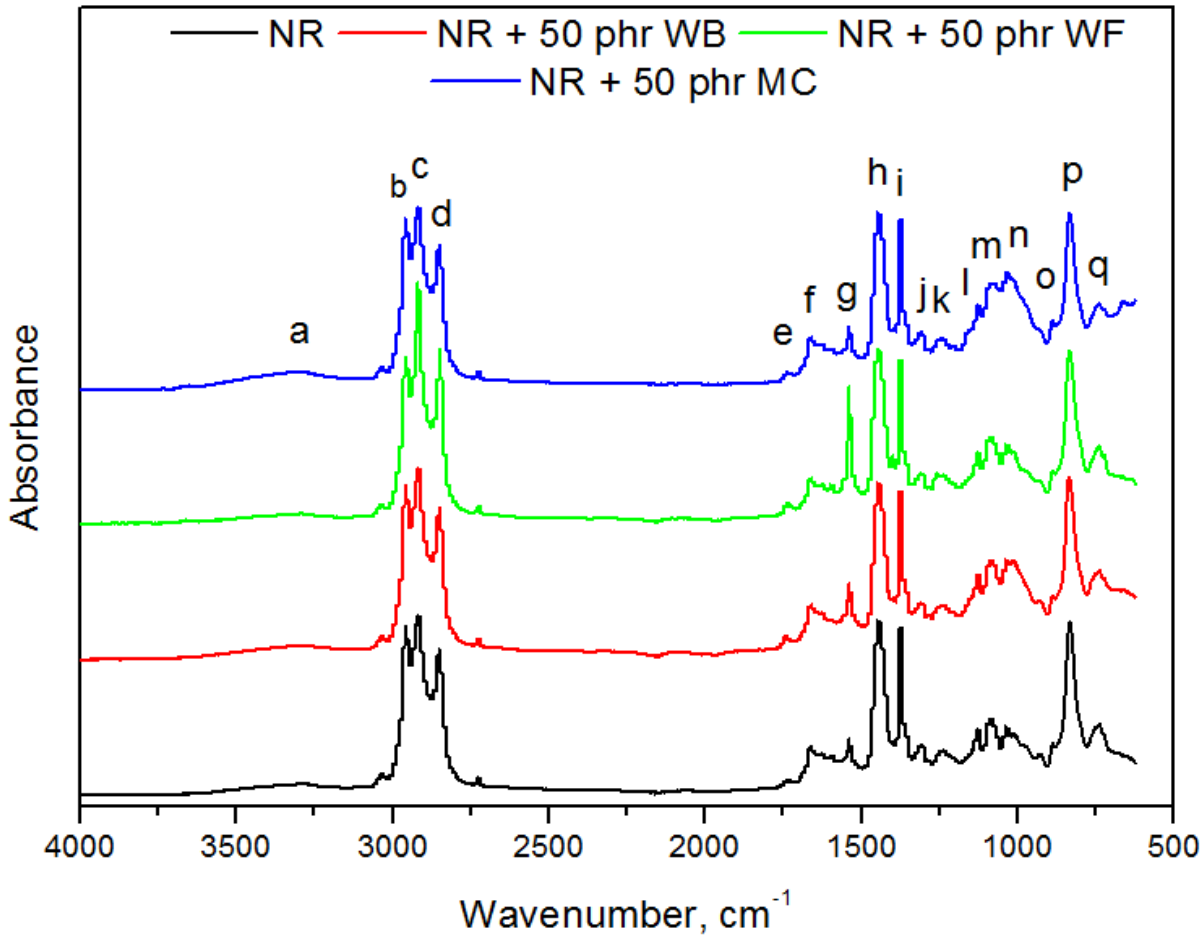

Figure 7. FTIR spectra of studied biocomposites

In the Fig. 7 there are presented FTIR spectra of analyzed biocomposites. Similarities in spectra for all studied samples are related to their chemical composition. Small absorption band (a) characteristic for stretching vibrations of hydroxyl groups was observed at 3300 cm^{-1} for NR/lignocellulose filler biocomposites. At the same time the absorption maxima at 3 290 cm^{-1} for unfilled NR was noticed. This suggests presence of proteins (monopeptides and dipeptides) in natural rubber (Manaila E, Stelescu MD, Doroftei F (2015) Polymeric composites based on natural rubber and hemp fibers. Iran. Polym. J. 24:135-148.). The bands (b, c and d) in the range of 2960-2850 cm^{-1} were attributed to the symmetric and asymmetric stretching vibrations of C-H bonds in CH_2 groups present in aliphatic elastomer chains and CH_3 end groups. Signals (e and f) around 1740 and 1660 cm^{-1} are associated with the stretching vibrations of unconjugated C=O and C=C bonds. Such bonds can be present in natural rubber after processing, but the intensity of responsible signals is slightly higher for modified samples, which is related to presence of such bonds in cellulose, hemicellulose and lignin, especially after partial degradation due to biocomposite processing (Budarin, V. L.,

Clark, J. H., Lanigan, B. A., Shuttleworth, P. and Macquarrie, D. J. 2010. Microwave assisted decomposition of cellulose: A new thermochemical route for biomass exploitation. *Bioresource Technol.* **101:**3776–3779). The absorption band (g) around 1540 cm^{-1} was related to the presence of C=C double bonds in material's structure. As it can be seen, the highest intensity of this band was observed for sample NR + 50 phr WF, which may be related to curing efficiency of this biocomposite. Signal (h) around 1450 cm^{-1} is associated with scission vibrations of C-H bonds in CH_2 groups in aliphatic chains. Absorption maxima (i) at 1375 cm^{-1} is related to the vibrations of C-H bonds in CH_3 end groups groups. Band (j) at 1309 cm^{-1} might be attributed to the OH groups plane deformation vibrations. Signal (k) at 1243 cm^{-1} and bands (l, m and n) in the range of 1125-1035 cm^{-1} can be associated with vibrations of C-O-C, C-O, C=C and C-C-O groups. Their intensity is strictly related to the incorporation of lignocellulose fillers and correlate with the high intensity of corresponding signals on spectra of used fillers. Absorption maximas (o, p and q) observed in the range of 890-740 cm^{-1} can be attributed to the bending vibrations of C-H bonds and skeletal vibrations of C-C bonds in aliphatic chains of elastomer.

3.5. Thermogravimetric analysis

Table 4. Thermal decomposition characteristics of prepared biocomposites.

Sample	Mass loss, %				T_{1max}, °C	T_{2max}, °C
	2	5	10	50		
	Temperature, °C					
WB	111.7	225.3	265.3	336.8	309.4	-
WF	188.8	263.3	288.8	364.7	-	373.3
MC	175.6	288.5	311.1	360.4	-	367.4
NR	264.8	320.7	349.8	392.7	-	388.0
NR + 50 phr	193.4	262.8	292.0	386.6	310.4	388.1
NR + 50 phr	209.6	280.0	310.8	386.4	-	385.0
NR + 50 phr	208.4	285.2	321.6	382.7	-	374.7

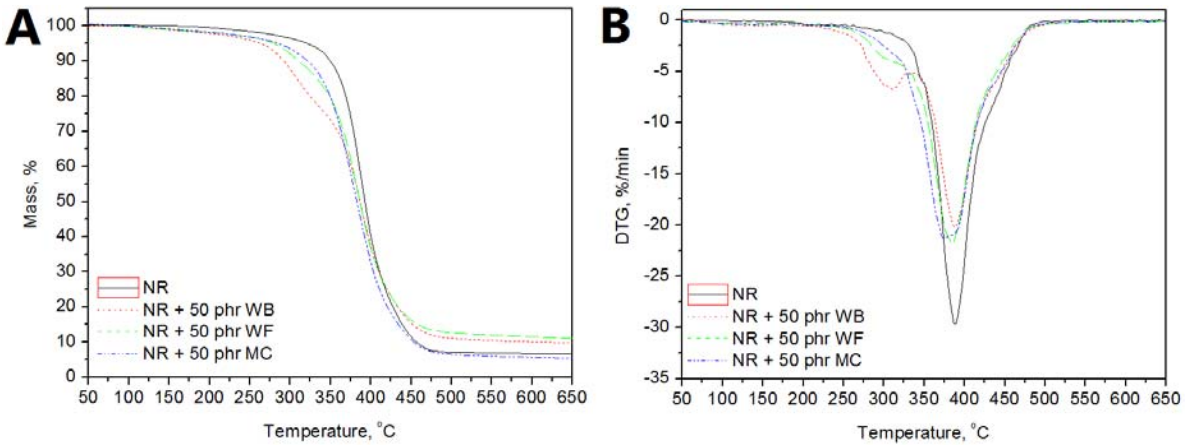

Figure 8. TGA and DTG curves determined for biocomposites.

The results of the thermogravimetric analysis of natural rubber based biocomposites are presented in Fig. 8 and summarized in Table 4. Presented data indicate significant decrease of the thermal stability with the addition of lignocellulose fillers, which is related to the rather poor thermal stability of used fillers in comparison to neat NR matrix. Moreover, noticeable differences have been observed between samples filled with WB and other fillers. Such phenomenon is associated with different chemical composition of applied biofillers. Wheat bran, except cellulose, contain also significant amounts of hemicellulose, lignin and other compounds and according to literature reports, decomposition of hemicellulose and lignin occurs in lower temperature range in comparison to cellulose [Chapple S, Anandjiwala R (2010) Flammability of natural fiber-reinforced composites and strategies for fire retardancy: A review. J. Thermoplast. Compos. 23:871-893]. Hemicellulose and lignin present in cell walls of wheat bran begin to decompose even before reaching 150 °C, while decomposition of the cellulose, resulting in formation of volatiles and char starts around 200 °C [Fan M, Naughton A (2016) Mechanisms of thermal decomposition of natural fiber composites. Compos Part B: Eng. 88:1-10.].

As it can be seen in differential thermogravimetric (DTG) curves, for sample NR + 50 phr WB, there is noticeable peak at 310.4 °C, related to the degradation of components present in wheat bran. Similar peak was observed in case of thermal degradation of pure wheat bran (309.4 °C). Samples NR + 50 phr WF and NR + 50 phr MC only one peak is observed on DTG curves, due to the overlapping of peaks characteristic for natural rubber and cellulose present in wood flour and microcellulose, however it can be seen that addition of lignocellulose fillers shifts position of peak towards lower temperatures. Such signal is very characteristic for cellulose materials, which show rapid mass loss around 360 °C [Ming G,

Qui-ju D (2006) Studies on the thermal degradation of cellulosic fibers treated with flame retardants. The Chinese Journal of Process Engineering 6:242-246].

3.6. Dynamic mechanical analysis

In the Fig. 9 the influence of the type of lignocellulose filler on the storage modulus (E′) as a function of temperature is shown. The lowest values of E′ in the glassy region were observed for unfilled NR, while the highest values E′ in the glassy region were measured for sample NR + 50 phr MC. The values of E′ modulus correspond with the results of hardness and crosslink density of obtained biocomposites.

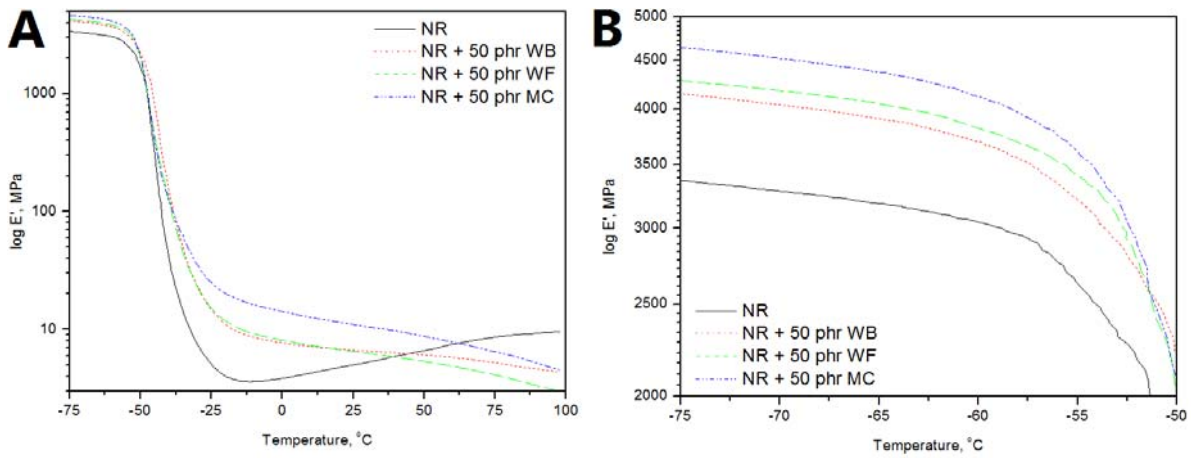

Figure 9. Storage modulus of biocomposites as a function of temperature.

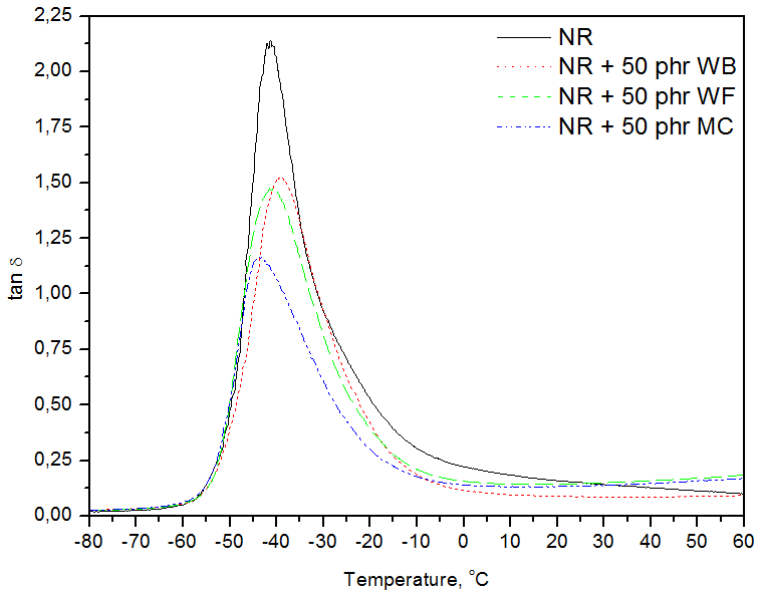

Figure 10. Plot of tanδ of biocomposites as a function of temperature.

The results of loss tangent (tanδ) as function of temperature are presented in Fig. 10. As it can be seen, addition of fillers not only shifts the temperature position of maximum value of tan δ peak, but also lowers the peak magnitude, which can be correlated with the reduced mobility of polymer chains at the matrix-filler interface. This indicates a better adhesion at the matrix-filler interface and is in agreement with previous studies (Cao et al. 2005; Sormana and Meredith, 2004; Tarakcilar, 2011). Bindu and Thomas, based upon the information and formulas presented by Abdalla and Kojima (Abdalla et al., 2007; Bindu and Thomas, 2013; Kojima et al., 1993), proposed a method for calculation of the amount of polymer chains immobilized through matrix-filler interaction in accordance with formula (11):

$$C_v = 1 - \frac{(1 - C_o)W}{W_o} \quad (11)$$

where C_v is the volume fraction of the immobilized polymer chains, C_o stands for the volume fraction of the immobilized chains in the pure natural rubber (taken to be 0), and W and W_o are energy loss fractions for analyzed sample and pure NR, respectively. Energy loss fraction W can be calculated from the tan δ in accordance to the following relation (12):

$$W = \frac{\pi \cdot \tan\delta}{\pi \cdot \tan\delta + 1} \quad (12)$$

Glass transition temperatures (T_g) and volume fractions (C_v) of immobilized polymer chains are presented in Table 5. Glass transition temperature of prepared composites (T_g) was determined as the position of maxima on the curve loss tangent (tan δ) versus temperature. For comparison, Tg as position of maxima on the curve loss modulus (E") versus temperature was also presented. It can be clearly seen that T_g and C_v values depends strongly on the characteristics of applied filler. The lowest C_v value were determined for composite containing wheat bran, which can be associated with chemical structure of this filler. Proteins (around 4 wt.%) present in WB may act like a plasticizers simultaneously enhancing the molecular motion in prepared composite [Hejna A, Formela K, Saeb MR (2015) Processing, mechanical and thermal behavior assessments of polycaprolactone/agricultural wastes biocomposites. Ind. Crop. Prod. 2015, 76:725-733.]. This phenomenon decrease porosity of obtained biocomposites (see Table 3), which affects glass transition temperature [Kasapis S, Sablani SS, Rahman MS, Al-Marhoobi IM, Al-Amri IS (2007) Porosity and the effect of structural changes on the mechanical glass transition temperature. J. Agric. Food Chem. 55:2459-2466.]. This explain the highest value of glass transition temperature in case of sample NR + 50 phr WB comparing to samples filled with WF or MC.

Table 5. Glass transition temperatures, volume fractions of immobilized polymer chains and adhesion factors of the biocomposites.

Properties	Sample			
	NR	NR + 50 phr WB	NR + 50 phr WF	NR + 50 phr MC
T_g (with respect to tanδ max,), °C	-41.19	-39.22	-41.50	-43.15
T_g (with respect to E" max.), °C	-48.48	-47.61	-49.48	-49.30
E' at 25 °C, MPa	5.00	6.67	6.51	11.01
tanδ at 25 °C	0.15	0.09	0.15	0.13
C_v	0	0.0498	0.0552	0.0977
A	-	0.0211	-0.0808	-0.3467

For better understanding the interfacial interactions between NR and used lignocellulose fillers, the adhesion factor (A) was calculated from dynamic mechanical analysis results (Wei et al., 2015). Kubát et al [Kubát, J., Rigdahl, M. and Welander, M. (1990), Characterization of interfacial interactions in high density polyethylene filled with glass spheres using dynamic-mechanical analysis. J. Appl. Polym. Sci., 39: 1527–1539.] assumed that the loss factor of the composite (tan δ_c) can be expressed in terms of volume fraction and mechanical damping of filler, interface and polymer matrix by presented formula (13):

$$\tan\delta_c = V_f \tan\delta_f + V_i \tan\delta_i + V_m \tan\delta_m \quad (13)$$

where c, f, i and m subscripts denote biocomposite, filler, interphase and matrix, while V is the filler volume fraction of each phase.

Assuming that the damping of the filler can be considered very low, because of its rigidity and the volume fraction of the interface is even lower and can be neglected comparing to its filler and matrix counterparts, formula (14) may be rearranged into:

$$\frac{\tan\delta_c}{\tan\delta_m} \cong (1-V_f)(1+A) \quad (14)$$

where adhesion factor is described by following formula (15):

$$\mathrm{A} = \left(\frac{V_i}{1-V_f}\right)\left(\frac{\tan\delta_i}{\tan\delta_m}\right) \quad (15)$$

Formula (15) could be rewritten and adhesion factor may be expressed in terms of the relative damping of biocomposite and pure polymer and the volume fraction of filler assuming that the transcrystallinity layer at the interphase may be neglected, because of the rather low fiber aspect ratio of applied fillers. Such rearrangement of the formula (16) leads to:

$$A = \left(\frac{1}{1-V_f}\right)\left(\frac{\tan\delta_c}{\tan\delta_m}\right) - 1 \quad (16)$$

A low value for A indicates high level of interface adhesion and enhanced interactions between the matrix and filler particles (Wei et al., 2013). The A values for analyzed samples are presented in Table 5. Adhesion factor values are in line with the presented values of C_v, which suggest the highest matrix-filler adhesion for samples containing MC and the lowest for NR/WB composite. Presented calculations explain the differences in static mechanical properties between studied biocomposites. Negative values of adhesion factor in case of samples containing wood flour and microcellulose can be associated with the simplification of model and neglecting of the filler anisotropy and development of the interphase region, which obviously have slight influence on the macromolecular mobility at the filler surroundings (Correa CA, Razzino CA, Hage E (2007) Role of maleated coupling agents on the interface adhesion of polypropylene-wood composites. J. Thermoplast. Compos. 20:323-338.).

3.7. Scanning electron microscopy

The influence of the type of lignocellulose filler on morphology of biocomposites is presented in the Fig. 11. Presented images demonstrate surface of biocomposites after extraction with toluene (72 h, at room temperature). Applied methodology allows effective assessment of voids formed during extraction, which are related to two factors. First of them is amount of soluble fraction (e.g. unbonded elastomer) present in biocomposites. The second factor affecting, is possible separation of lignocellulose filler from NR matrix due to permanent stress acting on NR matrix during swelling. This is associated with solvent absorption capacity of biocomposites, which is limited by matrix-filler interactions and cross-link density of biocomposites.

It was observed that MC was well-embedded in the natural rubber matrix, compared to WB and WF. Significant differences in dispersion is due to different particle size distribution of MC and WB or WF (see Figure 1). Particle sizes WB and WF were similar, however the morphology of biocomposties with these fillers was clearly different (Figures 10 B and C). This confirms significant influence of chemical composition on matrix-filler interactions. As mentioned before, wheat bran contain significant amount of starch, proteins or lipids, which can act like plasticizers in NR/WB biocomposites. Better dispersion of WB in NR matrix decrease porosity of NR/WB biocomposites. Furthermore, recently Jong [Jong L (2015) Toughness of natural rubber composites reinforced with hydrolyzed and modified wheat

gluten aggregates. J. Polym. Environ. 23:541-550.] proved that wheat gluten can act like reinforcement of natural rubber. This explain more developed surface in case of sample NR + 50 phr WB, comparing to NR + 50 phr WF. The presented SEM images confirm the results of curing characteristics, mechanical and thermal properties conducted in the obtained biocomposites.

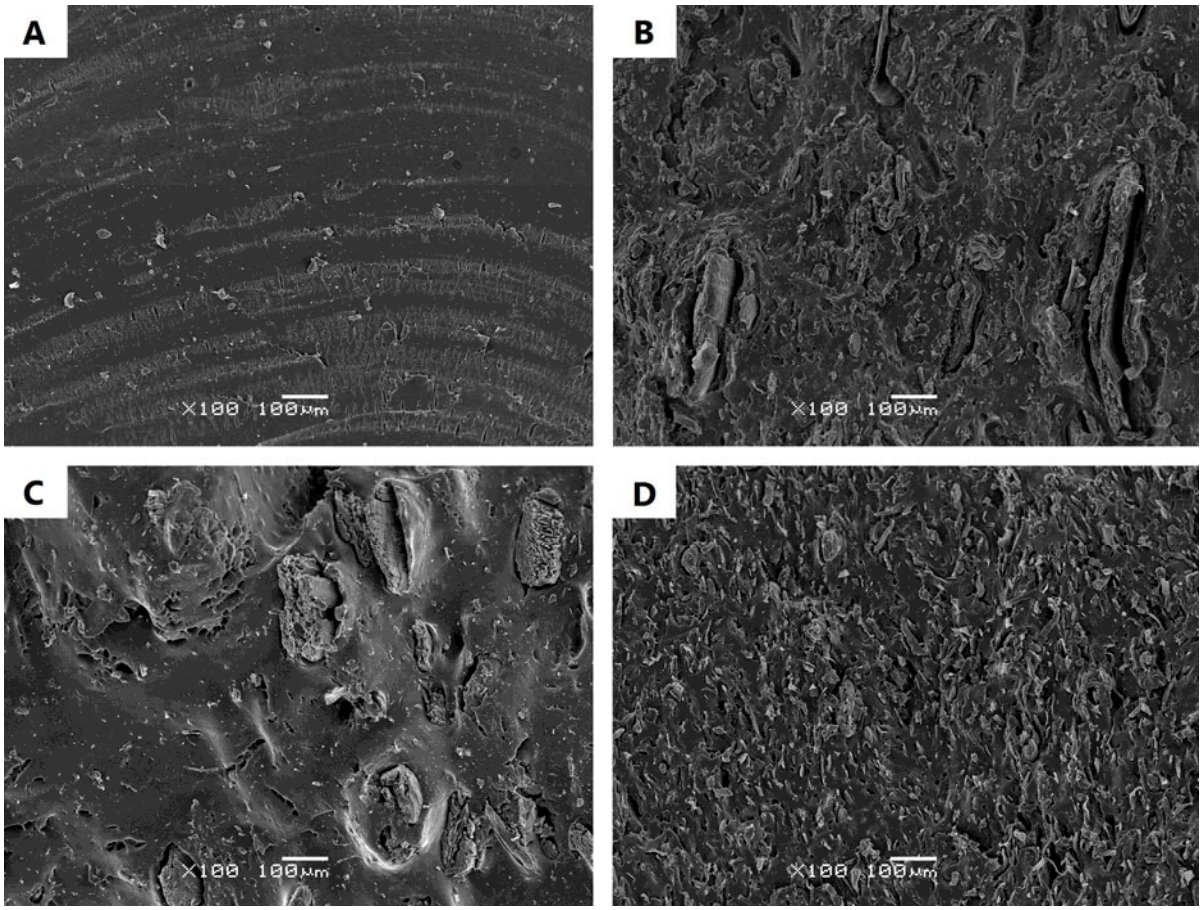

Figure 11. SEM images of biocomposites surface after swelling tests (magnification x100): A – unfilled NR; B – NR + 50 phr WB; C – NR + 50 phr WF; D – NR + 50 phr MC

4. Conclusions.

NR/WB biocomposites with different content of WB (10, 30 and 50 phr) were prepared in an internal mixer and followed by cross-linking with sulphur curing system. Furthermore, for better understanding of the interfacial interactions between NR and WB, the properties of the NR/WB biocomposites were compared with those filled with two commercial cellulosic fillers: wood flour (WF) and microcellulose (MC). Characteristics of applied cellulosic fillers was performed basing on particles size distribution, elemental analysis, WD-XRF and FTIR analysis. The results shown that particle size distribution and chemical composition of the lignocellulose filler have a significant influence on the processing, physico-mechanical, thermal and morphological properties of the studied biocomposites. Comparing to commercial cellulosic filler, WB filler content high amount of amino-acids, which act like

plasticizers having beneficial influence on processing, physical, thermo-mechanical and morphological properties of biocomposites. Furthermore, high content of macro- and microelements present in WB filler may affect in positive way on further biodegradation of biocomposites.

Reinforcing activity of applied cellulosic fillers was evaluated using a Wolff coefficient activity. The obtained results suggests reinforcing effect of cellulosic fillers increase with increasing content of filler. Although, the reinforcing activity of WB in NR based biocomposites was slightly lower comparing to commercial cellulosic fillers, which confirm partial plasticizing of NR with proteins present in wheat bran. It was noticed that reinforcing activity of cellulosic fillers are not corresponded with the results of mechanical properties, which can be related to strain inducted crystallization of NR matrix. Higher amount of cellulosic filler into NR matrix limited mobility of polymer chains, which was confirmed by the results of modulus at 100/300%, hardness, cross-linking density and dynamic mechanical analysis. Therefore strain-induced crystallization of NR matrix is very limited. This phenomenon explain negligible influence of chemical composition and particles size distribution of applied cellulosic fillers on static mechanical properties of highly filled (50 phr) NR biocomposites, which were comparable, regardless type of used filler.

It was noticed that addition of cellulosic fillers decrease thermal stability of biocomposites, which is due to poor thermal stability of used fillers in comparing to pure NR matrix. Therefore the stability of NR matrix, comparing to characteristics of used biofiller, has higher impact on thermal stability of biocomposites.

The SEM analysis showed that MC was well-embedded in the natural rubber matrix, compared to WB and WF, which is due to the smallest size particles of this filler. On the other hand, differences between morphology of NR/WB and NR/WF biocomposites are related to chemical composition of cellulosic filler. Present in WB proteins can act like as plasticizers, which allowing better dispersion of WB filler in NR matrix and reduce porosity of NR/WB biocomposites. This work confirmed that wheat bran can be successfully applied as low-cost alternative for “conventional” cellulosic fillers into elastomeric composites.

Furthermore, presented results indicate that further studies on that field should focus on: i) evaluation the impact of proteins, macro- and microelements present in cellulosic filler on biodegradation efficiency of biocomposites; ii) optimization of NR based biocomposites’ processing and curing conditions (e.g. applied curing system); iii) application of WB together with other fillers (e.g. nanofillers) as “hybrid fillers” in biocomposites.

References

Abdalla M, Dean D, Adibempe D, Nyairo E, Robinson P, Thompson G (2007) The effect of interfacial chemistry on molecular mobility and morphology of multiwalled carbon nanotubes epoxy nanocomposite. Polymer 48:5662-5670.

Agarwal UP, Reiner RS, Ralph SA (2010) Cellulose I crystallinity determination using FT-Raman spectroscopy: univariate and multivariate methods. Cellulose 17:721-733.

Bernardinelli OD, Lima MA, Rezende CA, Polikarpov I, deAzevedo ER (2015) Quantitative 13C MultiCP solid-state NMR as a tool for evaluation of cellulose crystallinity index measured directly inside sugarcane biomass. Biotechnol Biofuels 8:110.

Barth A (2007) Infrared spectroscopy of proteins. Biochim Biophys Acta 1767:1073-1101.

Berthet MA, Angellier-Coussy H, Machado D, Hilliou L, Staebler A, Vicente A, Gontard N (2015) Exploring the potentialities of using lignocellulosic fibres derived from three food by-products as constituents of biocomposites for food packaging. Ind Crop Prod 69, 110-122.

Bertran MS, Dale BE (1986) Determination of cellulose accessibility by differential scanning calorimetry. J Appl Polym Sci 32: 4241-4253

Bindu P, Thomas S (2013) Viscoelastic behavior and reinforcement mechanism in rubber nanocomposites in the vicinity of spherical nanoparticles. J Phys Chem B 117:12632-12648.

Błędzki AK, Franciszczak P, Mamun A (2014) The utilization of biochemically modified microfibers from grain by-products as reinforcement for polypropylene biocomposite. Express Polym Lett 10: 767-778.

Błędzki AK, Franciszczak P, Osman Z, Elbadawi M (2015) Polypropylene biocomposites reinforced with softwood, abaca, jute, and kenaf fibers. Ind Crop Prod 70:91-99.

Brüning K, Schneider K, Heinrich G (2012) Deformation and orientation in filled rubbers on the nano- and microscale studied by X-ray scattering. J Polym Sci Pol Phys 50:1728-1732.

Budarin VL, Clark JH, Lanigan BA, Shuttleworth P, Macquarrie DJ (2010) Microwave assisted decomposition of cellulose: A new thermochemical route for biomass exploitation. Bioresource Technol 101:3776-3779.

Cao X, Lee LJ, Widya T, Macosko C (2005) Polyurethane/clay nanocomposites foams: processing, structure and properties. Polymer 46:775-783.

Caprez A, Arrigoni E, Amadò R, Neukom H (1986) Influence of different types of thermal treatment on the chemical composition and physical properties of wheat bran. J Cereal Sci 4:233-239.

Chapple S, Anandjiwala R (2010) Flammability of natural fiber-reinforced composites and strategies for fire retardancy: A review. J Thermoplast Compos 23:871-893.

Chikhi M, Agoudjil B, Boudenne A, Gherabli A (2013) Experimental investigation of new biocomposite with low cost for thermal insulation. Energ Buildings 66:267-273.

Ciolacu D, Ciolacu F, Popa VI (2011) Amorphous cellulose - structure and characterization. Cellul Chem Technol 45:13-21.

Colom X, Carrillo F, Nogués F, Garriga P (2003) Structural analysis of photodegraded wood by means of FTIR spectroscopy. Polym Degrad Stab 80:543-549.

Correa CA, Razzino CA, Hage E (2007) Role of maleated coupling agents on the interface adhesion of polypropylene-wood composites. J Thermoplast Compos 20:323-338.

Datta J, Głowińska E (2011) Influence of cellulose on mechanical and thermomechanical properties of elastomers obtained from mixtures containing natural rubber. Polimery 56:823-827.
Faix O (1991) Classification of Lignins from Different Botanical Origins by FT-IR Spectroscopy. Holzforschung 45:21-27.
Faludi G, Dora G, Imre B, Renner K, Móczó J, Pukánszky B (2014) PLA/lignocellulosic fiber composites: Particle characteristics, interfacial adhesion, and failure mechanism. J Appl Polym Sci 131: 39902.
Fan M, Naughton A (2016) Mechanisms of thermal decomposition of natural fiber composites. Compos Part B: Eng 88:1-10.
Flory PJ, Rehner J (1943) Statistical mechanics of cross-linked polymer networks I. rubberlike elasticity. J Chem Phys 11:512-520.
Franciszczak P, Błędzki AK (2015) Tailoring of dual-interface in high tenacity PP composites – Toughening with positive hybrid effect. Compos Part A: Appl S doi:10.1016/j.compositesa.2015.07.001.
French AD (2014) Idealized powder diffraction patterns for cellulose polymorphs. Cellulose 21:885-896.
French AD, Cintrón MS (2013) Cellulose polymorphy, crystallite size, and the Segal crystallinity index. Cellulose 20:583-588.
Gao M, Dai QJ (2006) Studies on the thermal degradation of cellulosic fibers treated with flame retardants. The Chinese Journal of Process Engineering 6:242-246.
Georgiopoulos P, Kontou E (2015) The effect of wood-fiber type on the thermomechanical performance of a biodegradable polymer matrix. J Appl Polym Sci 132:42185.
Gurunathan T, Mohanty S, Nayak SK (2015) A review of the recent developments in biocomposites based on natural fibres and their application perspectives, Compos Part A: Appl S 77: 1-25.
Hejna A, Formela K, Saeb MR (2015) Processing, mechanical and thermal behavior assessments of polycaprolactone/agricultural wastes biocomposites. Ind Crop Prod 76:725-733.
Hong H, He H, Jia D, Zhang H (2011) Effect of wood flour on the curing behaviour, mechanical properties, and water absorption of natural rubber/wood flour composites. J Macromol Sci Part B Phys 50:1625-1636.
Horvath AL (2006) Structurally Complicated Materials: I. Wood. J Phys Chem Ref Data 35:77-92.
Ismail H, Edyham MR, Wirjosentono B (2002) Bamboo fibre filled natural rubber composites: the effects of filler loading and bonding agent. Polym Test 21:139-144.
Jacob M, Thomas S, Varughese KT (2004) Mechanical properties of sisal/oil palm hybrid fiber reinforced natural rubber composites. Compos Sci Technol 64:955-965.
Jiang C, He H, Jiang H, Ma L, Jia DM (2013) Nano-lignin filled natural rubber composites: Preparation and characterization. Express Polym Lett 7:480-493.
Jong L (2015) Toughness of natural rubber composites reinforced with hydrolyzed and modified wheat gluten aggregates. J Polym Environ 23:541-550.
Karaağaç B (2014) Use of ground pistachio shell as alternative filler in natural rubber/styrene–butadiene rubber-based rubber compounds. Polym Compos 35:245-252.

Kasapis S, Sablani SS, Rahman MS, Al-Marhoobi IM, Al-Amri IS (2007) Porosity and the effect of structural changes on the mechanical glass transition temperature. J Agric Food Chem 55:2459-2466.
Khan RA, Beck S, Dussault D, Salmieri S, Bouchard J, Lacroix M (2013) Mechanical and Barrier Properties of Nanocrystalline Cellulose Reinforced Poly(caprolactone) Composites: Effect of Gamma Radiation. J Appl Polym Sci 129:3038-3046.
Kojima Y, Usuki A, Kawasumi M, Okada A, Kurauchi T, Kamigaito O (1993) Sorption of water in nylon 6-clay hybrid. J Appl Polym Sci 49:1259-1264.
Korol J, Lenża J, Formela K (2015a) Manufacture and research of TPS/PE biocomposites properties. Compos Part B: Eng 68:310-316.
Korol J, Burchart-Korol D, Pichlak M (2015b) Expansion of environmental impact assessment for eco-efficiency evaluation of biocomposites for industrial application. J Clean Prod doi: 10.1016/j.jclepro.2015.11.101.
Kramárová Z, Alexy P, Chodák I, Špirk E, Hudec I, Košíková B, Gregorová A, Šúri P, Feranc J, Bugaj P, Ďuračka M (2007) Biopolymers as fillers for rubber blends. Polym Advan Technol 18:135-140.
Karimi K, Taherzadeh MJ (2016) Analytical methods in pretreatment of lignocelluloses: Composition, imaging, and crystallinity. Bioresource Technol. 200:1008-1018.
Kljun A, Benians TAS, Goubet F, Meulewaeter F, Knox JP, Blackburn RS (2011) Comparative Analysis of Crystallinity Changes in Cellulose I Polymers Using ATR-FTIR, X-ray Diffraction, and Carbohydrate-Binding Module Probes. Biomacromolecules 12:4121-4126.
Kraus GJ (1963) Swelling of filler-reinforced vulcanizates. J Appl Polym Sci 7:861-871.
Kubát J, Rigdahl M, Welander M (1990) Characterization of interfacial interactions in high density polyethylene filled with glass spheres using dynamic-mechanical analysis. J Appl Polym Sci 39:1527–1539.
Kwiecień I, Adamus G, Bartkowiak A, Kowalczuk M (2104) Synthesis and structural characterization at the molecular level of oligo(3-hydroxybutyrate) conjugates with antimicrobial agents designed for food packaging materials. Des Monomers Polym 17: 311-321.
Li X, Tabil LG, Oguocha IN, Panigrahi S (2008) Thermal diffusivity, thermal conductivity, and specific heat of flax fiber-HDPE biocomposites at processing temperatures. Compos Sci Technol 68:1753-1758.
Liu R, Peng Y, Cao J, Chen Y (2014) Comparison on properties of lignocellulosic flour/polymer composites by using wood, cellulose, and lignin flours as fillers. Compos Sci Technol 103:1-7.
López-Manchado MA, Herrero B, Arroyo M (2003) Preparation and characterization of organoclay nanocomposites based on natural rubber. Polym. Int 52:1070–1077.
Manaila E, Stelescu MD, Doroftei F (2015) Polymeric composites based on natural rubber and hemp fibers. Iran Polym J 24:135-148.
Menon ARR, Pillai CKS, Nando GB (1998) Vulcanization of natural rubber modified with cashew nut shell liquid and its phosphorylated derivative - a comparative study, Polymer 39:4033-4036.

Mohammed L, Ansari MNM, Pua G, Jawaid M, Islam MS (2015) A review on natural fiber reinforced polymer composite and its applications. Int J Polym Sci Article ID 243947.
Peltola H, Pääkkönen E, Jetsu P, Heinemann S (2014) Wood based PLA and PP composites: Effect of fibre type and matrix polymer on fibre morphology, dispersion and composite properties. Compos Part A: Appl S 61:13-22.
Proniewicz LM, Paluszkiewicz C, Wesełucha-Birczyńska A, Majcherzyk H, Barański A, Konieczna A (2001) FT-IR and FT-Raman study of hydrothermally degradated cellulose. J Mol Struct 596:163-169.
Raza MA, Ashraf MA, Westwood AVK, Jamil T, Ahmad R, Inamm A, Deen KM (2014) Maleated high oleic sunflower oil-treated cellulose fiber-based styrene butadiene rubber composites. Polym Compos doi: 10.1002/pc.23273.
Ren Y, Zhao R, Yao Q, Li Q, Zhang X, Zhang L (2015) Effects of plasticizers on the strain-induced crystallization and mechanical properties of natural rubber and synthetic polyisoprene. RSC Adv 5:11317-11324.
Sałasińska K, Ryszkowska J (2015) The effect of filler chemical constitution and morphological properties on the mechanical properties of natural fiber composites. Compos Interfaces 22:39-50.
Sareena C, Ramesan MT, Purushothaman E (2012a) Utilization of coconut shell powder as a novel filler in natural rubber. J Reinf Plast Compos 31:533-547.
Sareena C, Ramesan MT, Purushothaman E (2012b) Utilization of peanut shell powder as a novel filler in natural rubber. J Appl Polym Sci 125:232-234.
Saunders RM (1978) Wheat Bran: Composition and Digestibility. in: Spiller GA (ed), Topics in Dietary Fiber Research, 1st edn. Plenum Press, New York, pp 43-58.
Schwanninger M, Rodrigues JC, Pereira H, Hinterstoisser B (2004) Effects of short-time vibratory ball milling on the shape of FT-IR spectra of wood and cellulose, Vib Spectrosc 36:23-40.
Selmin F, Franceschini I, Cupone IE, Minghetti P, Cilurzo F (2015) Aminoacids as non-traditional plasticizers of maltodextrins fast-dissolving film, Carbohydr Polym 115:613-616.
Shen CH, Springer GS (1976) Moisture Absorption and Desorption of Composite Materials. J Comp Mater 10:2-20.
Shen L, Haufe J, Patel MK (2009) Product Overview and Market Projection of Emerging Biobased Plastics. Report No: NWS-E-2009-32 The Netherlands: Utrecht
Sobczak L, Brüggemann O, Putz RF (2013) Polyolefin Composites with Natural Fibers and Wood-Modification of the Fiber/Filler–Matrix Interaction. J Appl Polym Sci 127:1-17.
Sormana JL, Meredith JC (2004) High-Throughput Discovery of Structure-Mechanical Property Relationships for Segmented Poly(urethane−urea)s. Macromolecules 37:2186-2195.
Stein TM, Gordon SH, Greene RV (1999) Amino acids as plasticizers: II. Use of quantitative structure-property relationships to predict the behavior of monoammoniummonocarboxylate plasticizers in starch-glycerol blends. Carbohydr Polym 39:7-16.
Stein TM, Greene RV (1997) Amino acids as plasticizers for starch-based plastics. Starch 49:245-249.
Tarakcilar AR (2011) The effects of intumescent flame retardant including ammonium polyphosphate/pentaerythritol and fly ash fillers on the physicomechanical properties of rigid polyurethane foams. J Appl Polym Sci 120:2095-2102.

Teuber L, Osburg VS, Toporowski W, Militz H, Krause A (2016) Wood polymer composites and their contribution to cascading utilization. J Clean Prod 110:9-15.
Tomaszewska-Ciosk E, Golachowski A, Zdybel E (2013) Determination of biodegradation rate of carrier for microorganism immobilization fabricated based on starch. Pol J Chem Tech 15:110-114.
Wei L, Liang S, McDonald AG (2015) Thermophysical properties and biodegradation behavior of green composites made from polyhydroxybutyrate and potato peel waste fermentation residue. Ind Crop Prod 69:91-103.
Wei L, McDonald AG, Freitag C, Morrell JJ (2013). Effects of wood fiber esterification on properties, weatherability and biodurability of wood plastic composites. Polym Degrad Stab 98:1348-1361.
Xu F, Yu J, Tesso T, Dowell F, Wang D (2013) Qualitative and quantitative analysis of lignocellulosic biomass using infrared techniques: A mini-review. Appl Energy 104:801-809.
Yona AMC, Budija F, Kricej B, Kutnara A, Pavlic M, Pori P, Tavzes C, Petric M (2014) Production of biomaterials from cork: Liquefaction in polyhydric alcohols at moderate temperatures. Ind Crop Prod 54:296-301.
Yue Y, Han J, Han G, Zhang Q, French AD, Wu Q (2015) Characterization of cellulose I/II hybrid fibers isolated from energycane bagasse during the delignification process: Morphology, crystallinity and percentage estimation. Carbohyd Polym 133:438-447.
Zhou Y, Fan M, Che L, Zhuang J (2015) Lignocellulosic fibre mediated rubber composites: An overview. Compos Part B: Eng 76:180-191.